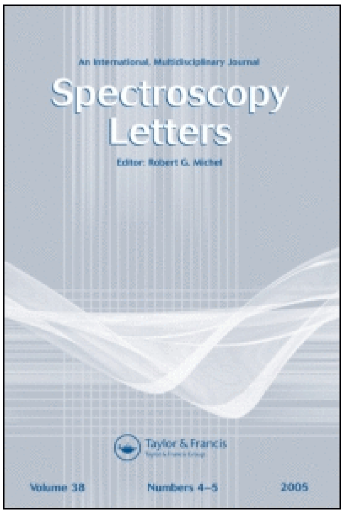

Spectroscopy Letters
Publication details, including instructions for authors and subscription information:
http://www.informaworld.com/smpp/title~content=t713597299

XAFS CHARACTERIZATION ON THE ACTIVE SITES OF Ni/γ-Al_2O_3 CATALYSTS FOR NO-SCR BY PROPENE

Ming[a]; Peiyan Lin[a]; Yilu Fu[a]
[a] Department of Chemical Physics, University of Science and Technology of China, Hefei, Anhui, People's Republic of China

To cite this Article Ming, Lin, Peiyan and Fu, Yilu(2001) 'XAFS CHARACTERIZATION ON THE ACTIVE SITES OF Ni/γ-Al_2O_3 CATALYSTS FOR NO-SCR BY PROPENE', Spectroscopy Letters, 34: 1, 83 — 92
To link to this Article: DOI: 10.1081/SL-100001454
URL: http://dx.doi.org/10.1081/SL-100001454

SPECTROSCOPY LETTERS, 34(1), 83–92 (2001)

XAFS CHARACTERIZATION ON THE ACTIVE SITES OF Ni/γ-Al_2O_3 CATALYSTS FOR NO-SCR BY PROPENE

Ming Meng, Peiyan Lin, and Yilu Fu

Department of Chemical Physics, University of Science
and Technology of China, Hefei, Anhui 230026,
People's Republic of China

ABSTRACT

Ni/γ-Al_2O_3 catalysts show high catalytic activity for the selective catalytic reduction of NO by C_3H_6. The microstructures of nickel species were characterized by the spectroscopy of X-ray Absorption Near Edge Structures (XANES) and Extended X-ray Absorption Fine Structures (EXAFS). The results of XANES and EXAFS indicate that the nickel species in the sample calcined at 500°C mainly exist as highly dispersed NiO phase, whereas in the samples calcined at 750 and 950°C, the nickel species mainly exist as $NiAl_2O_4$-like spinel. The surface $NiAl_2O_4$-like spinel is the main active site for the selective reduction of NO, and the highly dispersed NiO phase is the main active site for C_3H_6 oxidation. The formation of subsurface or bulk $NiAl_2O_4$ spinel results in the reduction of surface spinel and causes the decrease of activity for the selective catalytic reduction of NO by propene.

www.dekker.com

Key Words: Ni/γ-Al_2O_3 catalysts; XAFS; Characterization; NO-SCR

INTRODUCTION

The catalytic removal of nitrogen oxides (NO_x) in the presence of excess oxygen is one of the major and urgent projects in environmental catalysis. Although some ion-exchanged zeolite catalysts have been reported to be effective for lean NO_x removal, they normally show very low thermal stability (1–3). So, in the past several years, much attention has been attracted to oxides or the supported catalysts (4–11). Alumina supported oxides of Group VIII elements (Fe, Co, Ni) are active for NO-SCR by ethene (11). In these catalysts, Co/γ-Al_2O_3 catalysts have been investigated extensively (6–11), whereas few studies have been performed on Fe and Ni systems. Up to now, only the study by Okazaki and coworker indicates that the active sites for NO-SCR by ethene over Ni/γ-Al_2O_3 catalysts are aluminate phases (11), however, the microstructures of the active sites, such as the coordination symmetry, the surface dispersion, the length of Ni—O bond, and the interaction between nickel species and the support, are never investigated. X-ray Absorption Near Edge Structure (XANES) and Extended X-ray Absorption Fine Structure (EXAFS) are sensitive methods to explore the micro-structures of the absorbing atoms. In the present work, XANES and EXAFS techniques are employed to characterize the micro-structures of the active sites of Ni/γ-Al_2O_3 catalysts for NO-SCR by propene, the correlation between the structures and properties is elucidated.

EXPERIMENTAL

Sample Preparation

Ni/γ-Al_2O_3 catalysts (atomic ratio – Ni:Al = 5%) were prepared by adding γ-alumina to a given aqueous solution of nickel acetate. After drying at 120°C, the precursor was calcined in air at 350°C for 0.5 h to decompose the acetate, and then calcined at 500, 750, or 950°C for 4 h, respectively. The samples are denoted as Ni-Al-*X*, *X* stands for the calcination temperature (°C).

Evaluation of Catalytic Activity

The catalytic reaction was carried out in a gas-flow system with a microreactor. The reaction gas contained 1400 ppm NO, 1100 ppm C_3H_6, and 1.2% O_2 balanced by pure helium. The gas hourly space velocity (GHSV) is 12000 h^{-1}.

NO_x was analyzed by a chemiluminescence NO_x analyzer (Model 8840), and C_3H_6 was detected by a GC (Model SC-6) equipped with a FID detector.

X-Ray Diffraction (XRD)

X-ray diffraction measurement was carried out on a D/MAX-RA rotatory diffractometer, using Cu K_α as radiation source ($\lambda = 0.15418$ nm). The data were collected under the same conditions (40 kV and 100 mA).

X-Ray Absorption Fine Structure (XAFS)

The XAFS experiment was performed on the XAFS station, 4W1B beamline of Beijing Synchrotron Radiation Facility of National Laboratory (BSRF NL). The back-subtracted EXAFS functions were weighted by k^3 to compensate the diminishing amplitude, which resulted from the decay of the photoelectron wave. The structural parameters of the samples were obtained by curve-fitting method, using NiO and $NiAl_2O_4$ as model compounds.

RESULTS AND DISCUSSION

The Catalytic Activities

The activities of Ni/γ-Al_2O_3 catalysts for the selective catalytic reduction of NO by C_3H_6 are shown in Figure 1. From Figure 1A, it can be seen that the sample Ni-Al-750 possesses highest activity for NO selective reduction at the same reaction temperature. The maximum NO conversion over Ni-Al-750 is about 14% higher than that over Ni-Al-500. While for C_3H_6 oxidation, as shown in Figure 1B, sample Ni-Al-500 possesses highest activity, and the oxidation activity decreases continuously with the increase of the calcination temperature. The temperature for 100% conversion of C_3H_6 over Ni-Al-950 is about 60°C higher than that over Ni-Al-500. The surface areas of the samples calcined at 500, 750, and 950°C are 113, 92, and 59 m^2/g, respectively. The decrease of the oxidation activity of the samples is consistent with the reduction of the surface area, which implies that the sintering of active phases or support may be an important reason for the decrease of the oxidation activity. But for NO reduction, activity is not directly proportional to the surface area. For the samples calcined at 500 and 750°C, with the elevation of calcination temperature the reduction activity increases, which suggests that the nickel phases in Ni-Al-750 and Ni-Al-500 are different.

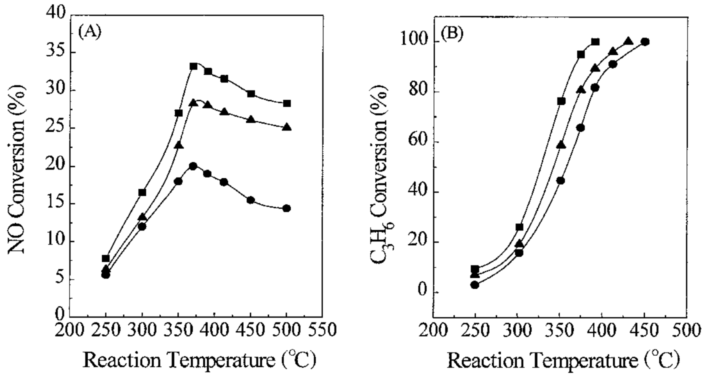

Figure 1. A) NO conversion versus reaction temperature over Ni/γ-Al_2O_3 catalysts calcined at different temperatures: (●) 500°C, (▲) 950°C, (■) 750°C. B) C_3H_6 conversion versus reaction temperature over Ni/γ-Al_2O_3 catalysts calcined at different temperatures: (●) 500°C, (▲) 950°C, (■) 750°C.

X-Ray Diffraction (XRD)

To characterize the active sites, the XRD spectra of the samples were recorded and are shown in Figure 2A. In each profile, there are a group of diffracted peaks appearing at $2\theta = 19.6°, 32.1°, 37.6°, 45.9°, 61.0°$, and $67.1°$, which are in good agreement with those of the support γ-Al_2O_3 (ASTM 10-425). The XRD spectra of the model compounds NiO and $NiAl_2O_4$ are also recorded and presented in Figure 2B. The diffracted peaks of NiO and $NiAl_2O_4$ appear at $2\theta = 37.3°, 43.3°, 63.0°, 75.5°, 79.5°$ and $2\theta = 19.0°, 31.4°, 37.0°, 45.0°, 56.0°, 59.7°$,

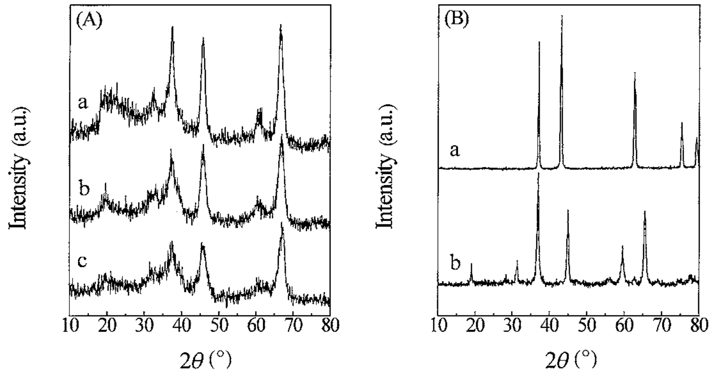

Figure 2. A) XRD spectra of Ni/γ-Al_2O_3 catalysts calcined at different temperatures: a) 950°C, b) 750°C, c) 500°C. B) XRD spectra of the model compounds: a) NiO, b) $NiAl_2O_4$.

65.6°, 77.8°, respectively. Compared with Figure 2A, it is found that only the peak at $2\theta = 37.3°$ of NiO is close to that at $2\theta = 37.6°$ of γ-Al_2O_3. The positions of all the other diffracted peaks of NiO and $NiAl_2O_4$ are different from those of γ-Al_2O_3, the 2θ difference is more than 0.5°. This means that the diffracted peaks in Figure 2A mainly correspond to γ-Al_2O_3. The possible phases regarding nickel in this case cannot be comfirmed by XRD method. Comparing the profiles of the samples calcined at different temperatures, it is easily found that the intensity of all the peaks increases remarkably with the elevation of the calcination temperature, which implies the gradual sintering of the support.

X-Ray Absorption Near Edge Structure (XANES)

Since XRD cannot give more useful information, XAFS method was employed to characterize the active sites. The XANES spectra of the samples and model compounds of Ni K-edge are presented in Figure 3A.

It is clear that all the XANES spectra of the samples and model compounds seem to be analogous to each other. At absorption edge, an obvious white line (1s→4p) is formed. However, comparing the spectra with each other in detail, some small difference can be found. Firstly, the white lines of the samples are disturbed by a very small asymmetric signal at the left side, which is normally resulted from the (1s→4s) migration (12). For the samples calcined at 750 and 950°C, it is more obvious. Secondly, at the postedge the signal intensities of the samples are different from each other. The higher calcination temperature, the

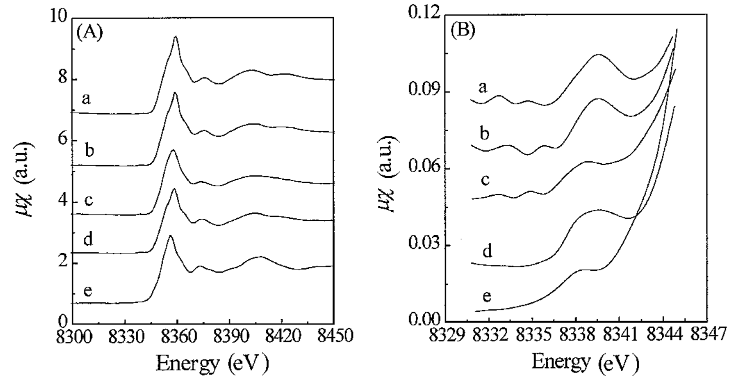

Figure 3. A) XANES spectra of Ni K-edge of the model compounds and Ni/γ-Al_2O_3 catalysts calcined at different temperatures: a) 950°C, b) 750°C, c) 500°C, d) $NiAl_2O_4$, e) NiO. B) The corresponding amplified XANES spectra of (A).

stronger oscillating signal. Thirdly, at the preedge, there is a very weak absorption peak corresponding to (1s→3d) migration (13). When the preedge part of the XANES spectra is amplified, this peak can be seen as in Figure 3B. It is clear that with the elevation of calcination temperature, the intensity of the corresponding peak of the samples is increasing. Comparing the spectra of the samples and model compounds, it is found that the spectrum of Ni-Al-500 is similar to that of NiO, whereas the spectra of Ni-Al-750 and Ni-Al-950 are close to that of $NiAl_2O_4$.

Extended X-Ray Absorption Fine Structure (EXAFS)

The k^3-weighted EXAFS oscillation functions of Ni K-edge of the model compounds and samples are presented in Figure 4A.

From Figure 4A, it can be seen that the EXAFS functions of model compounds NiO and $NiAl_2O_4$ are completely different. The EXAFS functions of Ni-Al-750 and Ni-Al-950 are very similar to that of $NiAl_2O_4$, however, the oscillating amplitudes of the samples are much lower. For Ni-Al-500, the EXAFS function seems to be more analogous to that of NiO. With the increase of the calcination temperature, the EXAFS functions of the samples become close to that of $NiAl_2O_4$, at the positions of $k = \sim 40$ and ~ 80 nm^{-1}, the oscillating peaks gradually split into two peaks, and the oscillating amplitudes increase and tend toward that of $NiAl_2O_4$. These features show that the coordination environment of Ni atoms in the samples calcined at different temperatures are different. In Ni-Al-500, the nickel may exist mainly as NiO, whereas in Ni-Al-750 and Ni-Al-950, it may exist mainly in the form of $NiAl_2O_4$ or $NiAl_2O_4$-like phase.

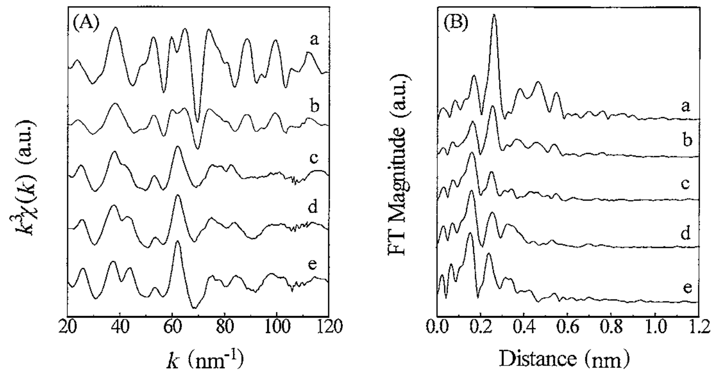

Figure 4. A) Ni K-edge EXAFS functions of the model compounds and Ni/γ-Al_2O_3 catalysts calcined at different temperatures: a) NiO, b) 500°C, c) 750°C, d) 950°C, e) $NiAl_2O_4$. B) The corresponding radial structure functions of the model compounds and catalysts in (A).

The corresponding radial structure functions (RSFs) of Ni K-edge of the samples and model compounds are shown in Figure 4B. For NiO, there are two coordination peaks appearing at 0.166 and 0.254 nm (uncorrected), considering the phase scattering shift, these two peaks could be assigned to Ni–O (0.209 nm) and Ni–Ni (0.296 nm) shells in NiO. For $NiAl_2O_4$, there are also two peaks, but the corresponding distances 0.159 and 0.245 nm (uncorrected) are smaller than those of NiO. Additionally, the FT magnitudes of the two peaks for NiO and $NiAl_2O_4$ are different. For NiO the second peak is much stronger than the first one, whereas for $NiAl_2O_4$ the intensity sequence is inverse because in the second shell in $NiAl_2O_4$ the Ni^{2+} ions mainly coordinate to Al^{3+} ions, which are light backscattering atoms. From both the peak positions and FT magnitudes, the RSFs of Ni-Al-750 and Ni-Al-950 are very close to that of $NiAl_2O_4$, which implies the similar coordination environment of Ni species in these two samples and the model compound $NiAl_2O_4$ even though the RSF of Ni-Al-500 is similar to that of NiO. All these results are in good agreement with those of XANES.

To quantitatively analyze the nickle phase in the samples, curve-fitting was performed on the first shell of the samples, the standard functions of amplitude and phase shift were taken from the corresponding shell of the model NiO and $NiAl_2O_4$. For Ni-Al-750 and Ni-Al-950, the first shell could be well fitted using $NiAl_2O_4$ as a model compound. According to the study by Arean and Vinuela (14), in $NiAl_2O_4$ spinel (AB_2O_4 structure), ~84% of Ni^{2+} ions occupy the B sites, and the rest Ni^{2+} ions occupy the A sites. The structural parameters of model $NiAl_2O_4$ are calculated on their result. For Ni-Al-500, the first shell could not be fitted by mono-shell fitting, no matter NiO or $NiAl_2O_4$ is used as a model compound. So, two-shell fitting was performed on the first shell of Ni-Al-500, which is described elsewhere (15). All the fitting results are listed in Table 1.

Table 1. The Structural Parameters of the First Shell (Ni–O) in the Samples[a]

	Ni–O Shell in NiO			Ni–O Shell in $NiAl_2O_4$			NiO–$NiAl_2O_4$
Sample	R_A (nm)	N_A	$\Delta\sigma_A^2$ (nm^2)	R_B (nm)	N_B	$\Delta\sigma_B^2$ (nm^2)	(molar ratio)
Ni-Al-500	0.208	4.1	0.000057	0.184	4.0	0.000049	~3:1
Ni-Al-750				0.183	5.1	0.000042	
Ni-Al-950				0.183	5.4	0.000033	
$NiAl_2O_4$[b]				0.183	5.7		
NiO[b]	0.209	6.0					

[a] R: coordination distance; N: Coordination number; $\Delta\sigma^2$: Debye–Waller factor.

[b] The structural parameters of $NiAl_2O_4$ and NiO are calculated on Refs. (14 and 16), respectively.

From Table 1, it can be seen that in Ni-Al-750 and Ni-Al-950 the coordination distance of Ni—O shell is almost the same as that of $NiAl_2O_4$. This means that the nickel in these two samples exists as $NiAl_2O_4$- or $NiAl_2O_4$-like spinel. While in Ni-Al-500, most of the nickel exists as NiO phase, only a small part of nickel (~1/4) exists as $NiAl_2O_4$- or $NiAl_2O_4$-like spinel. Comparing the coordination number of the samples and model compounds, it is found that the nickel species in Ni-Al-500 are in highly dispersed state. With the elevation of calcination temperature, the highly dispersed NiO phase gradually converts into $NiAl_2O_4$ spinel, the corresponding coordination number is also increasing, which suggests the growth of the particle size of $NiAl_2O_4$ or $NiAl_2O_4$-like phase. Although EXAFS results indicate that some nickel in Ni-Al-500 exist as spinel phase, the lower coordination number of Ni-O shell shows that this phase is mainly the highly dispersed surface spinel. According to the studies (13), the Ni^{2+} cations have a preference to occupy the surface octahedral sites of γ-Al_2O_3, at 500°C or lower temperature, the interaction between nickel species and the support is not very strong, most of Ni species still exist as NiO. However, with the increase of calcination temperature, the interaction becomes much stronger. Some Ni^{2+} cations diffuse into the subsurface or the bulk lattice of γ-Al_2O_3, occupying the octahedral sites and finally forming subsurface or bulk $NiAl_2O_4$ spinel. Apparently, the surface spinel phase in Ni-Al-950 must be less than that in Ni-Al-750. This may be related to the decrease of NO conversion.

Combined with the results of catalytic activities, it is clear that the activity for C_3H_6 oxidation of the samples depends on the amount of the highly dispersed NiO phase, whereas the activity for the selective catalytic reduction of NO is mainly related to the surface $NiAl_2O_4$-like phase. So, it is believed that the highly dispersed NiO are the main active sites for C_3H_6 oxidation, and that the surface $NiAl_2O_4$-like spinel are the main active sites for the selective catalytic reduction of NO. The increase of the reduction activity and the decrease of the oxidation activity are resulted from the change of dispersed NiO into $NiAl_2O_4$-like spinel. As to the lower NO conversion over Ni-Al-950 than that over Ni-Al-750, the sintering of the support, the growth of particle size of $NiAl_2O_4$-like spinel, and the diffusion of Ni^{2+} cations into subsurface or bulk of the sample are plausible explanations.

ACKNOWLEDGMENTS

This work was financially supported by National Natural Science Foundation of China (No. 29973037) and Anhui Natural Science Foundation (No. 99045429). The help from Dr. Li Xiao in activity determination is gratefully acknowledged.

REFERENCES

1. Petunchi, J.O.; Hall, W.K. Effects of Selective Reduction of Nitric Oxide on Zeolite Structure. Appl. Catal. B **1994**, *3*, 239.
2. Cowan, A.D.; Dumpelmann, R.; Cant, N.W. The Rate-Determining Step in the Selective Reduction of Nitric oxide by Methane over a Co-ZSM5 Catalyst in the Presence of Oxygen. J. Catal. **1995**, *151*, 356.
3. Parvulescu, V.I.; Grange, P.; Delmon, B. Catalytic Removal of NO. Catal. Today **1998**, *46*, 233.
4. Shimizu, K.; Kawabata, H.; Satsuma, A.; Hattori, T. Formation and Reaction of Surface Acetate on Al_2O_3 during NO Reduction by C_3H_6. Appl. Catal. B **1998**, *19*, L87.
5. Kung, M.C.; Park, P.W.; Kim, D.W.; Kung, H.H.; Lean, NO*x* Catalysis over Sn/γ-Al_2O_3 Catalysts. J. Catal. **1999**, *181*, 1.
6. Okazaki, N.; Tsuda, S.; Shiina, Y.; Tada, A. Selective Removal of Cobalt Oxide from Cobalt-Loaded Alumina Catalysts and its Effect on the Activity for Selective Catalytic Reduction of Nitrogen Monoxide by Ethene in Excess Oxygen. Chem. Lett. **1998**, 51.
7. Meng, M.; Lin, P.Y.; Fu, Y.L. The Catalytic Removal of CO and NO over Co-Pt(Pd, Rh)/γ-Al_2O_3 Catalysts and their Structural Characterizations. Catal. Lett. **1997**, *48*, 213.
8. Hamada, H.; Kintaiki, Y.; Sasaki, M.; Ito, T.; Tabata, M. Transition Metal-Promoted Silica and Alumina Catalysts for the Selective Reduction of Nitrogen Monoxide with Propane. Appl. Catal. **1991**, *75*, L1.
9. Hamada, H.; Haneda, M.; Kakuta, N.; Miura, H.; Inami, K.; Nanba, T.; Hua, Q.W.; Ueno, A.; Ohfune, H.; Udagawa, Y. Effects of Co Ion Dispersion upon Selective Catalytic Reduction of NO over CoO/Al_2O_3 Catalysts. Chem. Lett. **1997**, 887.
10. Yan, J.Y.; Kung, M.C.; Sachtler, W.H.; Kung, H.H. Co/Al_2O_3 Lean NO_x Reduction Catalyst. J. Catal. **1997**, *172*, 178.
11. Okazaki, N.; Katoh, Y.; Shiina, Y.; Tada, A.; Iwamoto, M. Selective Suppression of Undesirable Competitive Oxidation during Selective Catalytic Reduction of Nitrogen Monoxide by Ethene in Excess Oxygen over Metal-Loaded Alumina. Chem. Lett. **1997**, 889.
12. Van Nordstrand, R.A. *Non-Crystalline Solids*; New York: Wiley, 1958.
13. Greegor, R.B.; Lytle, F.W.; Chin, R.L.; Hercules, D.M., Investigation of Supported Cobalt and Nickel Catalysts by X-Ray Absorption Spectroscopy. J. Phys. Chem. **1981**, *85*, 1232.
14. Arean, C.O.; Vinuela, J.S. Structural Study of Copper-Nickel Aluminate ($Cu_xNi_{1-x}Al_2O_4$) Spinels. J. Solid State Chem. **1985**, *60*, 1.

15. Lu, K.Q.; Wan, J. Extended X-Ray-Absorption Fine Structure of a System of Mixed Phases. Phys. Rev. B **1987**, *35*(9), 4497.
16. Sasaki, S.; Fujino, K.; Takeuchi, Y. X-Ray Determination of Electron-Density Distributions in Oxides MgO, MnO, CoO and NiO, and Atomic Scattering Factors of Their Constituent Atoms. Proc. of the Japan Acad. **1979**, *55*, 43.

Received June 7, 2000
Accepted August 1, 2000

Downloaded At: 03:13 30 January 2011

Request Permission or Order Reprints Instantly!

Interested in copying and sharing this article? In most cases, U.S. Copyright Law requires that you get permission from the article's rightsholder before using copyrighted content.

All information and materials found in this article, including but not limited to text, trademarks, patents, logos, graphics and images (the "Materials"), are the copyrighted works and other forms of intellectual property of Marcel Dekker, Inc., or its licensors. All rights not expressly granted are reserved.

Get permission to lawfully reproduce and distribute the Materials or order reprints quickly and painlessly. Simply click on the "Request Permission/Reprints Here" link below and follow the instructions. Visit the U.S. Copyright Office for information on Fair Use limitations of U.S. copyright law. Please refer to The Association of American Publishers' (AAP) website for guidelines on Fair Use in the Classroom.

The Materials are for your personal use only and cannot be reformatted, reposted, resold or distributed by electronic means or otherwise without permission from Marcel Dekker, Inc. Marcel Dekker, Inc. grants you the limited right to display the Materials only on your personal computer or personal wireless device, and to copy and download single copies of such Materials provided that any copyright, trademark or other notice appearing on such Materials is also retained by, displayed, copied or downloaded as part of the Materials and is not removed or obscured, and provided you do not edit, modify, alter or enhance the Materials. Please refer to our Website User Agreement for more details.

Order now!

Reprints of this article can also be ordered at

http://www.dekker.com/servlet/product/DOI/101081SL100001454